

Online Detection of Faulty Battery Cells in Energy Storage Systems Via Impulse Response Method

Morgan M. Kiani

Texas Christian University

m.kiani@tcu.edu

Abstract: Just-in-time detection of anomalies in automotive batteries can prohibit a viral propagation of the problem within the energy storage system. Given the cost associated with replacement of energy storage system in electric and hybrid electric vehicles, an effective condition monitoring can translate to substantial savings and reduced downtime. In this paper a condition monitoring technique based on the impulse response of the electrochemical batteries has been proposed. This method is capable of detection of abnormal operating characteristics in battery cells within an energy storage system while the unit is performing its intended function. Simulation and experimental results are provided to illustrate the practicality of the proposed method.

I. INTRODUCTION

Energy storage system forms an integral part of the electric (EV), hybrid electric (HEV), and plug-in hybrid electric vehicles (PHEV). The ultimate commercial success of these modern automobiles depends, in large, to development of a compact, reliable, and durable energy storage system. It is commonly accepted that while power electronics and electric propulsion motors have reached acceptable performance grades, energy storage systems are still far from optimal. In fact energy storage and power source elements (batteries and ultra capacitors) suffer from relatively high price of manufacturing, lack of compactness, and need for further reliability. Although an intensified research and development on development of electrochemical batteries is expected to result in lower cost, enhanced durability, and improved reliability, the need for development of an online condition monitoring in energy storage elements is far from exhausted.

Recent studies have indicated that malfunction and condition deterioration of battery cells within a matrix of batteries can propagate to other healthy elements and as such timely detection, treatment, or replacement of faulty batteries can impede the chance of a viral failure of the energy storage element [1],[2]. Among various signatures used for detection of state-of-charge (SOC) open circuit voltage, terminal impedance, equivalent electric circuit parameters, and frequency domain characteristics of the terminal quantities have been used [3],[4]. Most of these techniques can not be implemented while the energy storage system is operating. Impulse response technique introduced in [5] illustrates an effective tool for detection of SOC and potential faults within electrochemical batteries. Access to terminal quantities (i.e. current and voltage) and temperature for each cell is the only

required information. This information are usually available in the battery management system (BMS).

In this paper, by defining current as input and cell voltage as the output, the impulse response of the battery at various SOC levels are captured. These impulse responses are then transformed in the form of an ARMAX model. Using real time measurement of electric current and convolution theory the expected terminal voltage of each cell is calculated and then is compared to the actual measured voltage. Using this comparison, occurrence of any anomaly is detected. One of the most useful application of this method is to detect the battery cells which are in need of balancing. Using balancing techniques a longer life time for the battery cell and its neighboring cells can be achieved. The online nature of the proposed technique along with the absence of need for sophisticated measurement equipment makes it suitable for mass production and integration into the battery management systems.

II. MODELING OF ELECTROCHEMICAL BATTERIES USING IMPULSE RESPONSE

If the state of charge, temperature, and the terminal currents of an electrochemical battery vary within a reasonably small range, a linear time invariant approximation for battery is acceptable. Given the fact that the state of charge and temperature vary reasonably slow and the linear range of operation with respect to the terminal current is sufficiently wide, development of a linear time invariant model for the electrochemical batteries seems appropriate. Impulse response is a powerful tool for time domain analysis of linear and piecewise linear time invariant systems. To extract the impulse response a sufficiently narrow pulse of current with an area of “unity” should be applied to the terminals of the battery (battery needs to be at rest) and the terminal voltage is captured. The terminal voltage can be expressed as the sum of open circuit voltage and the transient voltage caused by the impulse current, i.e:

$$V_{batt} = V_{oc}(SOC, T) + V_{tr}(SOC, T) \quad (1)$$

$$V_{batt} = V_{oc}(SOC, T) + i_{\delta}(t) * h_{\delta}(SOC, T) \quad (2)$$

In which $i_{\delta}(\cdot)$, $h_{\delta}(\cdot, \cdot)$, and $*$ stand for impulse current, impulse response at a given SOC and temperature, and convolution respectively. The width of the current pulse is required to be sufficiently small as compared to the smallest time constant of the battery. Given the fact that the electrochemical time constants of the battery are influenced by the speed of chemical reactions, no practical limitation on

power electronic-based implementation of the impulse currents are foreseen. Figure 1 illustrates variations of the terminal voltage for sealed lead-acid and Li-ion batteries when a repetitive load has been placed across the terminals of the batteries. One can notice the gradual decrease of the open circuit voltage which is an indicator of the reduction in state of charge in the battery. Once the battery is depleted below certain limit, a much faster drop of the voltage takes place. This leads to an unstable scenario which eventually will damage the battery in future charging and applications. Therefore a discharge below certain SOC is not recommended for automotive applications.

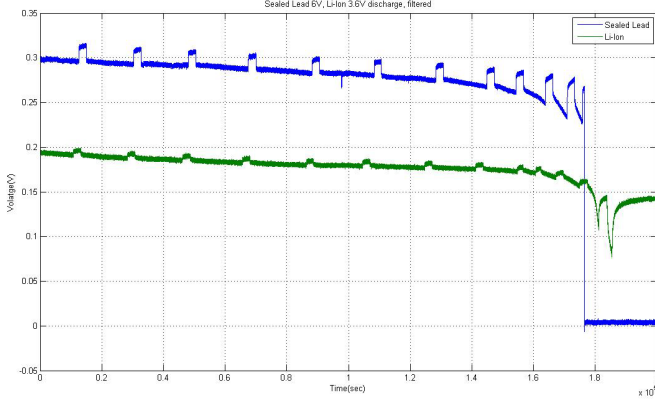


Figure 1: Discharging curve of a 6 Volts Sealed Lead-Acid Battery and 3.6 Volts Li-ion Battery over 2.8 hours.

Models based on the equivalent circuit of a battery have been vastly used in the past to develop an analytical model for the terminal readings. Figure 2 illustrates a commonly used equivalent circuit for an electrochemical battery.

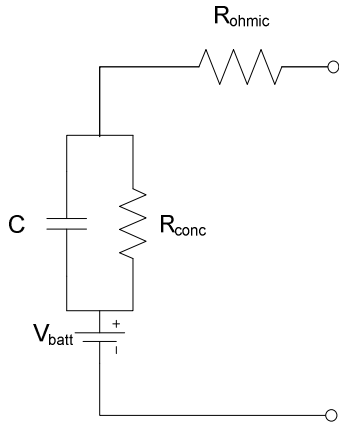


Figure 2: Equivalent circuit of an electrochemical battery

In which V_{batt} , C , R_{conc} , and R_{ohmic} represent the no-load voltage of the battery, double layer capacitance, internal resistance and galvanic resistance of the battery terminal respectively. These parameters are sensitive to the SOC and temperature. This intuitively suggests that the impulse response of the battery will depend upon SOC and temperature as well. The terminal impedance of the battery is given by the following expression:

$$Z_{eq} = R_{ohmic} + \frac{R_{conc}}{R_{conc} \cdot C \cdot s + 1} \quad (3)$$

If “n” batteries are connected in series then the terminal impedance can be approximated by:

$$Z_{eq,n} = \sum_{i=1}^n R_{ohmic,i} + \sum_{i=1}^n \frac{R_{conc,i}}{R_{conc,i} \cdot C_i \cdot s + 1} \quad (4)$$

Parameters of the equivalent circuit of a single electrochemical battery can be computed by connecting and consequently disconnecting a load across the terminals of the battery as demonstrated experimentally in figure 3.

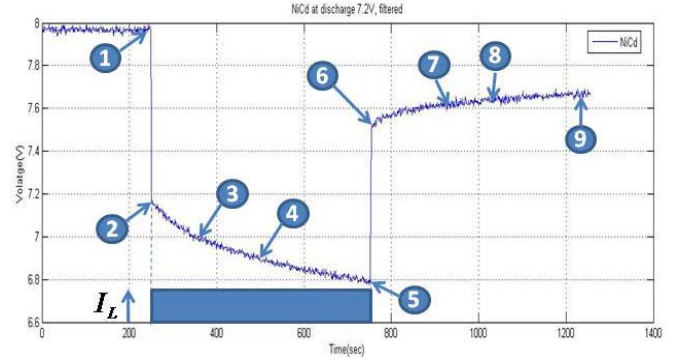


Figure 3: Detection of battery equivalent circuit parameters

Equations (5)-(7) can be used to identify the equivalent circuit parameters for a battery like the NiCd cell demonstrated in figure 3.

$$R_{ohmic} = \frac{V_1 - V_2}{I_L} \quad (5)$$

$$R_{conc} = \frac{V_9 - V_6}{I_L} \quad (6)$$

$$C = \frac{t_8 - t_7}{R_{conc} \cdot \ln(V_7/V_8)} \quad (7)$$

Alternatively one could use point (3) and (4) to obtain the equivalent circuit parameters. According to the equivalent circuit, the continuous domain impulse response of the battery can be approximated by:

$$H(s) = \frac{(R_{conc} \cdot R_{ohmic} s) + (R_{conc} + R_{ohmic})}{(1 + R_{ohmic} s)} \quad (8)$$

Which using a bilinear transformation can be transferred to a discrete time domain using the following expression in which the coefficients depend on the sampling time and parameters of the equivalent circuit :

$$H(q^{-1}) = \left(\frac{\alpha_1 q^{-1} + \alpha_0}{\beta_1 q^{-1} + \beta_0} \right) \quad (9)$$

It must be noted that the measurement noise should be carefully filtered out before such a model can be constructed. Furthermore, since the parameters in the equivalent circuit would vary as the temperature and the state of charge

changes, it is expected that the impulse response will also be a function of these conditions. Occurrence of the faults or aging effects in batteries will also alter the dynamics of the battery and as such the impulse response will exhibit changes. Figure 4 illustrates the impulse responses of a multi-cell Lithium-Ion battery at various state of charge superimposed on open circuit voltages of the battery. As can be seen the open circuit voltage of the battery varies with respect to the SOC. The sudden rise and fall of the voltage can be attributed to the double layer capacitor of the battery which acts as a short circuit during transients. Furthermore the time constants of the battery (tail part of the voltage) are arguably several times bigger than the length of the impulse current.

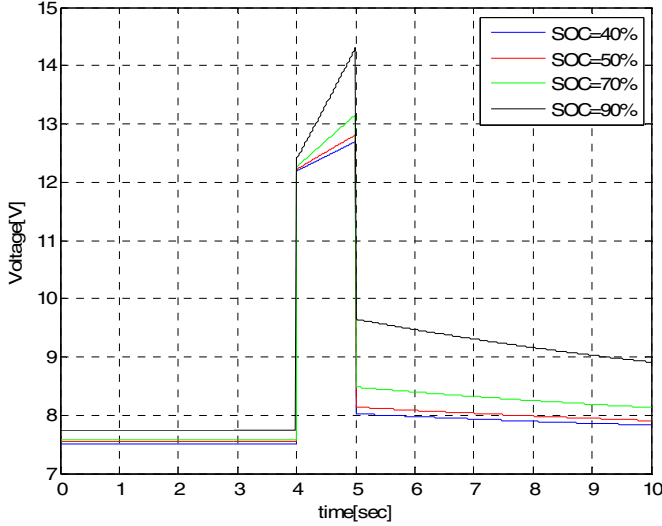


Figure 4: Impulse response of a multi-cell Lithium-Ion battery at various SOC levels

Once Impulse responses are captured using system identification tools an Autoregressive-moving average model (ARMAX) for the pair of input and output signals will be developed. This procedure will be repeated for various SOC and temperatures as needed. The ARMAX model can be symbolically presented as:

$$V_{tr}[k] = \frac{A(q^{-1})}{B(q^{-1})} i_{\delta}[k] + \frac{C(q^{-1})}{D(q^{-1})} e[k] \quad (10)$$

In which operator q^{-1} represents unit delay in discrete time domain and $e[k]$ denote the measurement noise (usually a white Gaussian noise is assumed). Figure 5 illustrates the comparison between the output of the ARMAX model and the actual voltage at a given state of charge. As can be noted there is good match between the calculated and actual voltages. A better match can be achieved by including higher orders of polynomial in the ARMAX model. However, to perform real time computations a compromise between level of matching and the corresponding computational cost has to be met. The existence of measurement error and noise will require higher dynamic orders. The first order model as represented in eqn. (9) represents an ideal case and depending on the quality of the sampling, sensing and data conversion

the accuracy of a first order model will be questionable. In the example shown in figure 5 the order of the A, B, C, and D are set at 20, 20, 2, and 20 respectively.

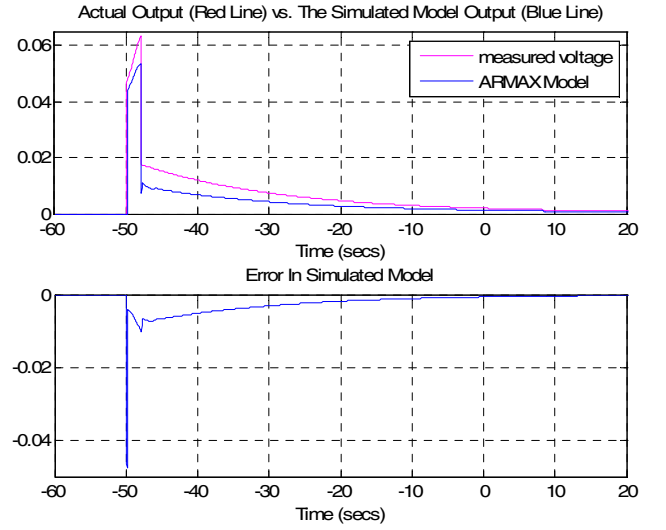


Figure 5: Comparison between the measured and calculated voltage (Top) and the resulting error in the simulated model (bottom) in a Li-Ion battery

III. DETECTION OF SOC AND FAULTS IN AN ENERGY STORAGE SYSTEM

Access to terminal quantities (i.e. current, temperature and voltage) for each cell or each group of cells within an energy storage element is usually provided through the battery management system. This information is used to detect the state of charge and state of health for each cell or group of cells [6]-[8]. In order to achieve this goal various impulse responses representing different SOC for the desired temperature will be convolved with the measured current to develop a family of predicted voltages. Among the computed waveform, the one with the closest proximity to the actual voltage will be chosen. The measure of “closeness” is usually a geometrical metric such as:

$$d = \lambda_1 \|V_{tr,\delta} - V_{tr,actual}\|_1 + \lambda_2 \|V_{tr,\delta} - V_{tr,actual}\|_2 \quad (11)$$

In which $\|\cdot\|_{1,2}$ represent the first and the second geometrical norms of the difference between the computed and measured transient voltages. While the first geometric norm can be used to identify the SOC for various cells, the second geometrical norm (i.e. representing the first time derivative of the waveform) will focus on detailed alteration of the voltage waveform caused by aging effects and potential faults. The weighting coefficients should be selected such that a mismatch between the average of the waveforms are detected first (i.e. $\lambda_1 \gg \lambda_2$). Once a sufficiently large mismatch has been observed then a more surgical effort for detection of the cause of the anomaly will be incorporated by giving more weight to the second norm (i.e. $\lambda_1 \ll \lambda_2$). Higher norms

can be incorporated to distinguish various types of faults if necessary[9]-[13]. In order to illustrate the effectiveness of the proposed method, a simple energy storage system comprised of four Li-ion battery cells have been developed in SimPower software (see figure 6). Figure 7 shows the predicted voltage for all four cells. The state of charge in the fourth cell was set at 40% while the other three cells were given a SOC of 90%. As can be observed using a periodic excitation of the package, the total predicted cell voltages have been captured and the best SOC has been automatically identified for the fourth cell. A more complex energy storage system consisting of several series and parallel circuits will be used next to further demonstrate the effectiveness of the proposed technique.

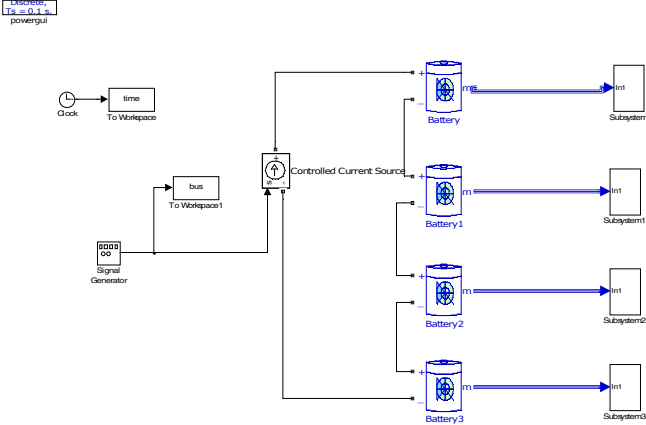


Figure 6: Schematic of the test model in Simpower

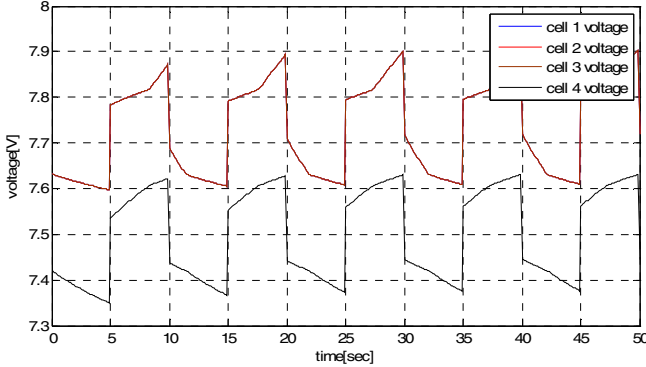


Figure 7 : Computed voltages along with the identified SOC Cell 1-3 with SOC=90%, Cell 4 with SOC 40%

In the second case study a matrix of Li-ion batteries with identical characteristics are put together forming “ n ” column and “ m ” rows. In this configuration the temperature, current, and voltage of each battery is measured. Figure 8 illustrates the circuit diagram and a picture of the hardware. The main task here is to monitor the state of charge and state of health in all batteries using the proposed technique. In order to accomplish this goal and in the first step first geometrical norm will be used. The impulse response for each column is defined as the sum of individual impulse responses for all batteries in that column, i.e.:

$$h_i[k] = \sum_{j=1}^n h_{i,j}[k] \Big|_{T=T_j} \quad i = 1 \cdots m \quad (12)$$

Consequently the pack voltage can be predicted as follows:

$$\hat{v}_i[k] = h_i[k] * i_i[k] \quad i = 1 \cdots m \quad (13)$$

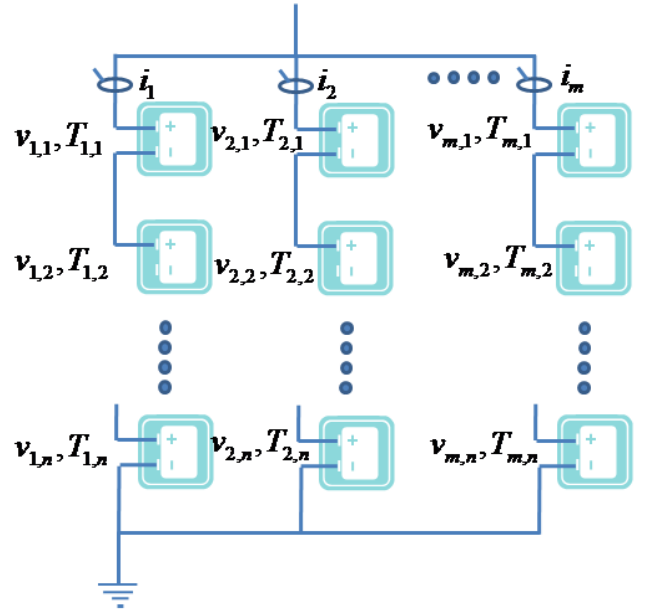
This value will be compared with the measured value of the pack voltage and relative measures of closeness will be recorded:

$$d_i = \frac{1}{N} \sum_{k=1}^N \left(\sum_{j=1}^n (v_{i,j}[k] - \hat{v}_i[k]) \right)^2 \quad i = 1 \cdots m \quad (14)$$

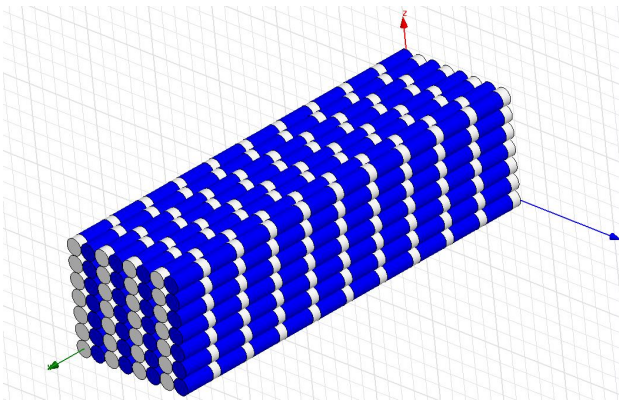
It must be noted that the window of recording for all terminal quantities (i.e. voltages and currents) has the same length of “ N ” samples. By setting thresholds for the measure of closeness one can monitor the occurrence of an anomaly in any column using the above calculation[14]. Once a column exhibit unusually high differences between the measured and computed voltages, this will be interpreted as an anomaly and all cells in that column will undergo a second monitoring, i.e.:

$$\begin{aligned} \hat{v}_{i,l}[k] &= h_{i,l}[k] \Big|_{T=T_{i,l}} * i_i[k] \\ d_{i,l}^* &= \frac{1}{N} \sum_{k=1}^N (v_{i,l}[k] - \hat{v}_{i,l}[k])^2 \quad i = 1 \cdots m \end{aligned} \quad (15)$$

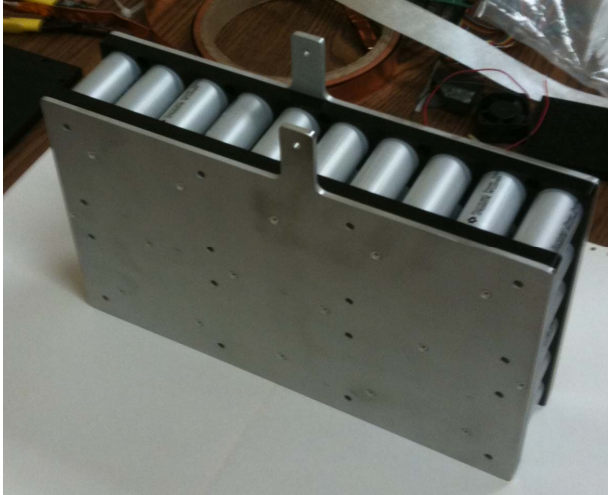
Where “ l ” denotes the order of the selected column with anomaly from the previous step. In this step a vertical search among the cells on the column with the problem is performed to find the cell or cells that contribute to this anomaly. Once they are detected then a further investigation incorporating higher order norms can be performed to distinguish the type of fault or aging effects in addition to adoption of the SOC.



(a) Circuit diagram of the case study



(b) Schematic of the battery package

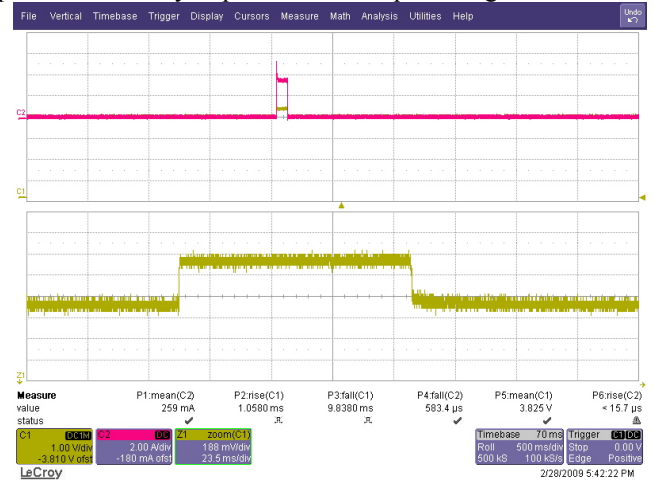


(c) Hardware implementation

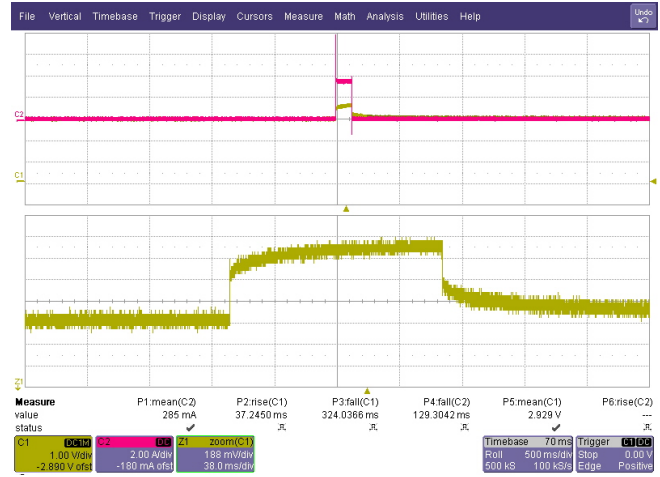
Figure 8: the circuit diagram, model, and hardware implementation of a Li-ion package

To validate the method a battery with a state of charge of 25% was included along with batteries which have a SOC of 90%. Figure 9 illustrates the impulse responses of these batteries. As can be clearly seen the sensitivity of the voltage with the low SOC to an injection of current is much higher than the one with high SOC. These impulse responses were used along with various location for the battery with low SOC within the matrix and each time the location was detected correctly. The time necessary for monitoring of all sensors (one voltage and one temperature per battery cell as well as one current sensor per parallel path) in a package with 60 batteries (6 parallel path) considering the necessary conditioning and filtering is less than 10mSec. The time necessary for selection of the impulse responses and computation to detect the location of the faulty battery is less than 20 [msec]. This means the overall monitoring and detection of the faulty cell will be less than 30[msec] using two TMS320F2812 dsp controllers. Additional memory in the battery management system will be necessary to store the impulse responses. The computational time can vary depending on number of anomalies and level of detection (in this study only low SOC was targeted). However, considering the operation of batteries in stationary and automotive applications the monitoring method is fast enough to detect the vast majority of the potential faults. Slow arcing

phenomenon will be studied separately due to its fast escalation. Usually this monitoring will take place in reasonable periods of time, however close monitoring of fast phenomenon may require a more frequent diagnostics.



(a) SOC=90%



(b) SOC=25%

Figure 9: Impulse responses of the Li-ion batteries with 90% and 25% SOC

IV. CONCLUSIONS

A new technique for real time condition monitoring of automotive and stationary batteries within a large energy storage system has been introduced. The same technique can be used for large stationary energy storage system used in flexible power systems. Impulse responses of the batteries at various SOC and temperatures have been used along with the terminal measurements to develop the proposed health monitoring system. It is expected that the proposed just-in-time control to improve the reliability and durability of the automotive and stationary battery energy storage systems by allowing for just in time detection and treatment of faulty batteries which would have otherwise escalated a viral propagation of the deterioration among the neighboring healthy battery cells. Accurate positioning of the faulty batteries will further simplify the repair of the energy storage system.

REFERENCES

1. Szumanowski, Y. Chang, "Battery Management System Based on Battery Nonlinear Dynamics Modeling", *IEEE Trans. Veh. Technol.*, Volume 57, Issue 3, pp. 1425-1432, 2008.
2. Tsenter, "Battery Management for Hybrid Electric Vehicle and Telecommunication Applications", *IEEE The 17th Annual Battery Conf. on Application and Advances*, pp. 233-237, 2002.
3. K.S. Ng, C. S. Moo, Y. P. Chen, Y. C. Hsieh, "State-of-charge estimation for lead-acid batteries based on dynamic open-circuit voltage", *IEEE 2nd Int. Power and Energy Conf., PECon'08*, pp. 972-976, Dec. 2008.
4. J. Chiasson, "Estimating the state of charge of a battery", *Proceeding of the IEEE American Control Conference*, vol. 4, pp. 2863-2868, June 2003.
5. Banaei, A. Khoobroo, B. Fahimi, "Online Detection of terminal voltage in Li-ion Batteries via Battery Impulse Response", *IEEE Int. Conf. Vehicle Power and Propulsion, VPPC'09*, pp. 194-198, Sept. 2009.
6. C. S. C. Bose, F. C. Laman, "Battery state of health estimation through Coup De Fouet", *IEEE The 2nd Annual of Telecommunications Energy Conference, INTELLEC'00*, pp. 597-601, 2000.
7. F. Olivier, M. Didier, "Testing battery state of health with portable metering devices?", *IEEE The 9th Annual of Telecommunications Energy Conference, INTELLEC'07*, pp. 203-209, 2007.
8. S. Brown, N. Mellgren, M. Vynnycky and G. Lindbergha, "Impedance as a tool for investigating aging in Lithium-ion porous electrodes, II. Positive electrode examination", *J. Electrochem. Soc.*, Vol. 155, 2008.
9. M. Kerala, R. Kostecki, "Interfacial impedance study of Li-ion composite cathodes during aging at elevated temperatures", *J. Electrochem. Soc.*, Vol. 153, No. 9, pp. A1644-A1648, 2006.
10. F. Huet, "A review of impedance measurements for determination of the state-of-charge or state of health of secondary batteries", *J. Power Sources*, Vol. 70, pp. 59-69, 1998.
11. C. S. C. Bose, D. Wilkins, S. McCluer, M. J. Model, "Lessons learned in using ohmic techniques for battery monitoring", *IEEE The 6th Battery Conference on Applications and Advantages*, pp. 99-104, 2001.
12. H. Yang, C. M. Huang, C.L.Huang, "Identification of ARMAX Model for Short Term Load Forecasting: An Evolutionary Programming Approach", *Power Systems, IEEE Transactions on*, Volume 11, No. 1, pp. 403-408, 1996.
13. A. Banaei, A. Khoobroo, B. Fahimi, "Online detection of terminal voltage in Li-ion batteries via battery impulse response", *IEEE International Conference on Vehicle Power and Propulsion, VPPC'09*, pp. 1-6, 2009.
14. M. Ragsdale, J. Brunet, B. Fahimi, "A Novel Battery Identification Method Based on Pattern Recognition", *IEEE International Conference on Vehicle Power and Propulsion, VPPC'08*, pp. 1-6, 2008.